Selective Cell Adhesion

DOI: 10.1002/anie.201109144

Cell Adhesion Behavior on Enantiomerically Functionalized Zeolite L Monolayers**

*Jehad El-Gindi, Kathrin Benson, Luisa De Cola, Hans-Joachim Galla, and Nermin Seda Kehr**

Dedicated to Professor Dieter Hoppe on the occasion of his 70th birthday

Most cell functions, such as adhesion, growth, proliferation, and differentiation, are affected by the way cells interact with extracellular matrix (ECM).[1] The ECM is a complex mixture of nonliving material that surrounds most of the cells in multicellular organisms and determines the physical properties of tissue by cell–matrix contacts. Apart from the regulation of the intercellular communication, ECM is responsible for the dynamic behavior of cells. In biomedical research, functionalized nanostructured materials, such as self-assembled monolayers (SAMs) of nanoparticles (NPs), have been used as a model system of ECM.[2] In the SAMs of NPs, the functional groups anchored to the NPs offer a much higher density than the same groups just covalently linked to the surfaces or as a SAM on the substrate.[2f,3] This effect leads to a higher number of contact points between cells and a surface, and so the information transfer between the living cell and the biocompatible material can be improved and controlled.

During the last decade it was shown that the interaction between cells and nanostructured surfaces can be controlled with bioactive ligands,[4] for example carbohydrates[5] or peptides[6] adsorbed or grafted to the surface,[7] thus introducing biocompatibility and enhancing cell adhesion and growth. Since in nature enantiomers show different effects on biological processes, both optical isomers of the respective bioactive ligands must be considered for the design of biocompatible nanostructured materials. In pioneering work, Addadi et al. showed that epithelial cells on an enantiomorphous calcium tartrate crystal surfaces have different behaviors.[8] Recently Sun et al. reported the interaction of living systems with chiral surfaces.[9] They demonstrated that cells change their morphology and their adhesion behavior depending on the used chiral surface. The same group reported that single- and double-stranded DNA and proteins have different adsorption behavior on enantiomorphous surfaces.[10]

Herein we present the enantioselective functionalization of zeolite nanoparticles with amino acids. Monolayers of these functionalized crystals were made, and the stereocontrolled interactions of the obtained enantiomorphous SAM with different cell types (primary cells, cell lines, including cancerogenic cells) are reported. The use of zeolites versus the simple functionalization of the substrate surface allows us to take advantage of the pores of the particles, which can host fluorescent dyes. Using enantiomorphous SAMs of dye-loaded zeolites allows us to establish the positioning of the cells on the NPs. Interestingly we found that our strategy can be employed for the separation of primary cells and cancerogenic cells. In particular, outstanding selectivity was found between endothelial and C-6-glioma cells, which were successful explored to separate the two types of cells.

Zeolite L crystals, which are well-known microporous aluminosilicate materials, were chosen as micro/nano objects, taking advantage of their crystalline nature, biocompatibility, optically transparency, and size-tunable properties[11] (30 to 10000 nm); particularly relevant for our application is the fact that their aspect ratio can be modulated from long cylinders up to very flat disks. Zeolites have many applications in the field of sensing,[12] electronics,[13] and biotechnology.[14] The surface of the crystals can be easily functionalized and they can be organized in monolayers on a silica substrate.[15,16] Recently, we described the functionalization of zeolites and SAM of zeolites with the bioactive molecules arginine–glycine–aspartic acid (RGD)[17] and α-D-mannoside,[18] respectively, by the microcontact printing technique. The corresponding SAMs of zeolites were used for cell-adhesion and cell-patterning experiments.[17,18]

Penicillamine (PEN), which is a bioactive chelating agent, was selected as bioactive molecule, as the two enantiomers possess very different properties. The pharmaceutical form of PEN is D-penicillamine (D-PEN), which is used to remove excess copper associated with Wilson's disease. L-penicillamine (L-PEN) inhibits the action of pyridoxine, which assists in the balancing of sodium and potassium as well as promoting red blood cell production.

Disk-shaped zeolite L crystals were prepared[11] with circa 820 nm average diameter and 360 nm height (see Figure 1 a,b; for a size distribution histogram and X-ray powder diffraction pattern (XRD) of the zeolites, see the Supporting Information, Figure S1 and S2, respectively). The crystals were loaded with *N*,*N*′-bis(2,6-dimethylphenyl)perylene-3,4,9,10-tetracarboxylic acid diimide (DXP), which is a fluorescent dye

[*] Dr. J. El-Gindi, Prof. L. De Cola, Dr. N. Seda Kehr
Physikalisches Institut and Center for Nanotechnology
Westfälische Wilhelms-Universität Münster
Heisenbergstrasse 11, 48149 Münster (Germany)
E-mail: seda@uni-muenster.de
K. Benson, Prof. H.-J. Galla
Institut für Biochemie, Westfälische Wilhelms-Universität Münster
Wilhelm-Klemm-Strasse 2, 48149 Münster (Germany)

[**] This work has been supported by ERC Advanced grant award no. 247365. N.S.K. thanks the SFB 858 for funding. We are grateful to Prof. Rainer Pöttgen and Dr. Manfred Möller for XRD measurements and Dr. Andreas Schäfer for XPS measurements.

Supporting information for this article is available on the WWW under http://dx.doi.org/10.1002/anie.201109144.

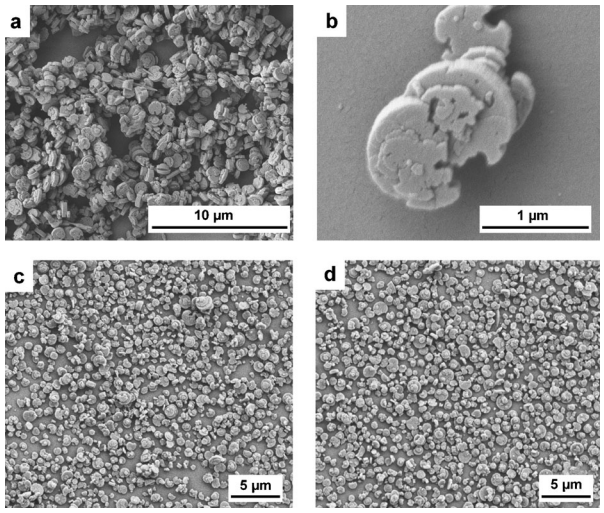

Figure 1. Scanning electron microscopy (SEM) images of disk-shaped zeolite L crystals (a,b). SEM images of L-PEN-zeo (c), D-PEN-zeo (d).

molecule,[19] and functionalized with 3-(aminopropyl)triethoxysilane (APTES) by standard procedures.[20] The amino-functionalized zeolite L crystals (NH_2-zeo) were divided into two parts. One part was functionalized with D-PEN and the other portion was reacted with L-PEN. The functionalization was conducted in the presence of 1-ethyl-3-(3-dimethylaminopropyl)carbodiimide (EDC) and *N*-hydroxysuccinimide (NHS) in dimethylsulfoxide (DMSO) to initiate the peptide coupling reaction, to introduce chirality on the zeolite surface (Supporting Information, Figure S3). Finally, the respective SAMs of enantiomerically functionalized zeolites (Figure 1c,d; for the preparation procedure, see the Supporting Information) on glass surfaces were prepared.[15a,16a] Zeolite L crystals were covalently attached on the glass surface to give stable SAMs of zeolite L.

The obtained D- and L-PEN functionalized zeolite crystals (D-PEN-zeo, L-PEN-zeo) were characterized by IR spectroscopy, X-ray photoelectron spectroscopy (XPS), and zeta potential. The IR bands of the ν(CO) and ν(CN) vibrations of the amide bonds of the PEN functionalized zeolite L, which are characteristic for amide I and amide II absorptions, were observed at about 1641 cm^{-1} and 1543 cm^{-1} (L-PEN-zeo) and 1645 cm^{-1} and 1543 cm^{-1} (D-PEN-zeo), respectively (Supporting Information, Figure S4,S5). The C 1s XPS spectra of the D- and L-PEN-zeo displayed a sharp C 1s peak at around 285.0 eV for the hydrocarbon chain. The binding energy of about 288.4 eV was assigned to the amide functions (O=C–N; Supporting Information, Figures S6, S7). Additionally, the significant increase of the zeta potential of the modified zeolites from 17.0 mV (NH_2-zeo) to 25.1 mV (D-PEN-zeo) and 24.9 mV (L-PEN-zeo), respectively, at pH 7 indicates the successful functionalization of the NH_2-zeo with penicillamine.

Subsequently, adhesion experiments were performed with different cell types, such as primary cells (endothelial cells), and cancerogenic cells (HeLa, RGC-5, RBE-4, C-6-glioma cells), on both D- and L-PEN-zeo monolayers. Each of the cell types were separately seeded on the D- and L-PEN-zeo monolayer on glass and incubated. After 12 h the adhered cells were washed, fixed and stained with 4′,6-diamidino-2-phenylindole dihydrochloride (DAPI).

Fluorescence microscope images showed that the adhesion behavior of cell lines as well as the primary cells is different on the functionalized zeolite L monolayers depending on the surface chirality (Figure 2). The population of HeLa cells (derived from cervical cancer), RBE-4 (rat brain

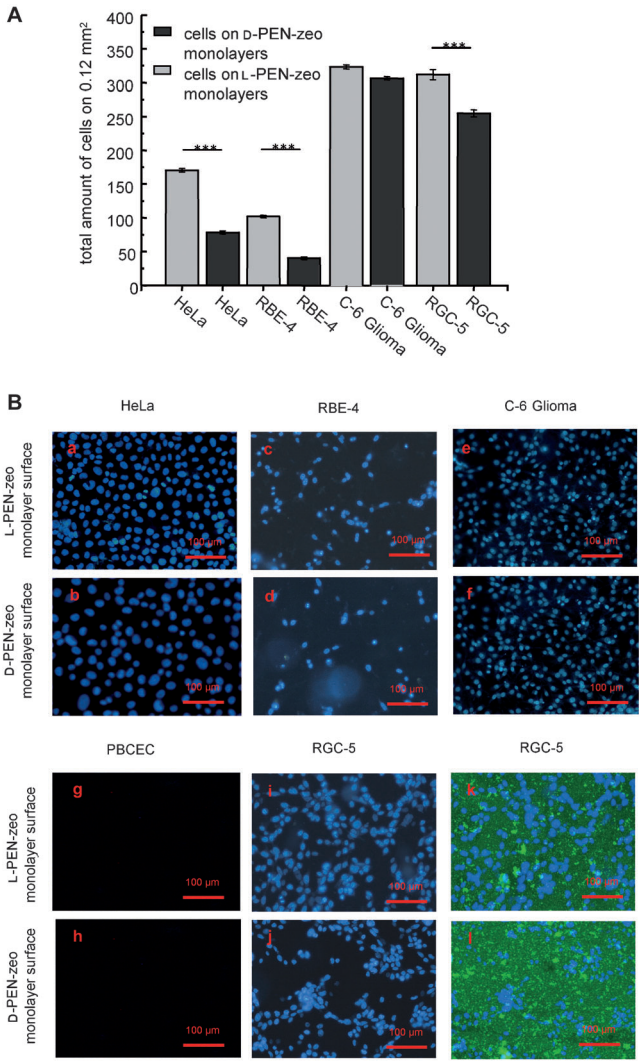

Figure 2. A) Quantitative data of adhered cells on D- and L-PEN zeolite monolayers. $N = 3$; *,*** data show significant differences (ANOVA: * $p \leq 0.05$, *** $p \leq 0.001$). Density of HeLa cells on SAMs of L-PEN-zeo and D-PEN-zeo was 1.4×10^5 cm^{-2} and 6.5×10^4 cm^{-2}, respectively. Density of RBE-4 cells on SAMs of L-PEN-zeo and D-PEN-zeo was determined to be 8.5×10^4 cm^{-2} and 3.3×10^4 cm^{-2}, respectively. Density of C-6-glioma cells on SAMs of L-PEN-zeo and D-PEN-zeo was 2.7×10^5 cm^{-2} and 2.5×10^5 cm^{-2}, respectively. Density of RGC-5 cells on SAMs of L-PEN-zeo and D-PEN-zeo was 2.6×10^5 cm^{-2} and 2.1×10^5 cm^{-2}, respectively. B) Fluorescence microscope images of different adhered cells on enantiomerically pure functionalized zeolite monolayer surfaces. (a–j) excitation range 330–385 nm; (k, l) excitation range 400–440 nm; blue: DAPI-stained cells, green: DXP-loaded zeolites.

endothelial cell line), and RGC-5 cells (rat retinal ganglion cell line) on the L-PEN-zeo surface was higher than on the D-PEN-zeo surface (Figure 2). For HeLa cells, more than twice as many cells adhered to the L-PEN-functionalized surface, and in the case of RBE-4 cells even close to three times more cells were detected. RGC-5 cells preferred the L-Pen-zeo surface but it looks like that this cell type build larger clusters on the D-Pen-zeo surface. These results demonstrate that cells can recognize and differentiate between different enantiomorphous SAM of zeolite surfaces. Impressive differences were obtained when we compared primary porcine brain capillary endothelial cells (PBCEC) and C-6-glioma cells (rat astrocyte glioma cells). The cells showed completely different adhesion behaviors. While C-6-glioma cells adhered on both surfaces almost equally, endothelial cells did not adhere at all (Figure 2). This behavior is probably caused by the bioactive substituents of the zeolite L surfaces[17,18] and/or is effected by the nanostructural character of the surfaces.[21] This striking result therefore would indicate that it is possible to separate one type of cell in the presence of the other. The use of DXP-loaded PEN zeolites allowed us to monitor zeolite crystals and the stained cells independently. We were able to determine the position of the cells on the monolayer surfaces. The fluorescence microscope images of RGC-5 cells on DXP-loaded SAMs of zeolites are shown as representative examples in Figure 2k,l.

Besides cell–ECM interaction, the analysis and the separation of cells (for example extraction of rare cells from a heterogeneous population) are important tools in experimental biology and medicine.[22] Especially prevention of contamination of cell cultures or separation of primary cells from cell lines require spatial methods. To show that the selectivity of our surface towards cell adhesion can be used for cell separation, we prepared our new enantiomorphous biocompatible material for a new set of experiments. As a representative example, we used D-PEN-functionalized zeolite monolayers to separate endothelial cells (primary cells) from C-6-glioma cells (cell line), because the isolation of differentiated glioma cells from endothelial cells of the blood–brain barrier (BBB) is still not possible by different digestion protocols. A 1:1 mixture of both cell types was seeded on the D-PEN-zeo monolayer, and after a 12 h incubation period, the supernatant and the D-PEN-zeo monolayer were separated. The adhered cells on the D-PEN-zeo monolayer were fixed and immunostained with antibodies. Van Willebrand factor (vWF, red fluorescence) expressed by endothelial cells[23] and glial fibrillar acid protein (GFAP, green fluorescence) expressed by C-6-glioma cells[24] were used as specific antigens. Subsequently nuclei of the adhered cells on the D-PEN-zeo monolayer were stained with DAPI (blue fluorescence). Finally they were analyzed by fluorescence microscopy (see Figure 3A) and quantified by using the program Image J (Figure 3B). The fluorescence image in Figure 3A clearly shows that C-6-glioma and endothelial cells are perfectly separated from each other by using D-PEN-zeo monolayer surfaces. The only cells that adhered on the zeolite monolayer were C-6-glioma cells, because only green fluorescent GFAP expressed cells were detected by fluorescence microscope. None of the red fluorescent vWF expressed endothelial cells were found on the surface of zeolite monolayers.

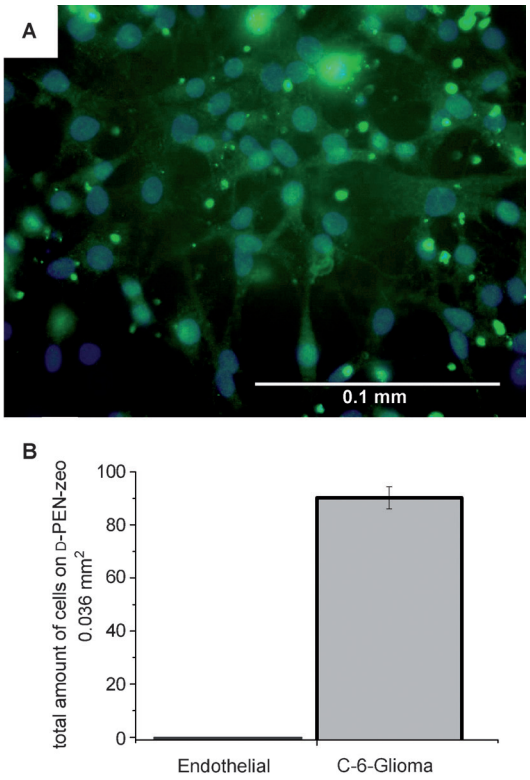

Figure 3. Separation of endothelial cells and C-6-glioma cells with SAM of D-PEN-zeo surfaces. A) The immunofluorescence image of the adhered GFAP-labeled C-6-glioma cells on SAMs of D-PEN-zeo surfaces (excitation range 460–550 nm; blue: DAPI stained C-6-glioma cells nucleus, green: GFAP-labeled C-6-glioma cells). B) Quantitative data of adhered cells on D-PEN-zeo monolayers. $N = 4$; * data show significant difference (ANOVA: * $p \leq 0.05$). Density of C-6-glioma cells on SAMs of D-PEN-zeo is 2.5×10^5 cm^{-2}. There were no endothelial cells on SAMs of D-PEN-zeo detected.

To improve our results, we quantified the number of non-adhered endothelial and C-6-glioma cells in the supernatant after the cell separation experiment. Cells in the supernatant were immunostained with vWF (endothelial cells) and GFAP (C-6-glioma cells), respectively, and analyzed by employing the enzyme-linked immunosorbent assay (ELISA). ELISA showed that in the supernatant of the cell separation experiment the amount of vWF (endothelial cells) was at least three times higher than the amount of GFAP (C-6-glioma cells; see Figure 4). Therefore our new enantiomorphous, biocompatible material (SAM of D-PEN-zeo) was able to absorb selectively in a first step more than 60% of the C-6-glioma cells from the starting 1:1 endothelial/C-6-glioma cell mixture.

In conclusion, we demonstrated the successful enantioselective functionalization of zeolites with D- and L-penicillamine, respectively, and the construction of the respective enantiomorphous SAM of zeolite surfaces. By cell adhesion experiments with different type of cells we demonstrated that cells recognize and differentiate between the different enantiomorphous SAM of zeolite surfaces. Finally we used

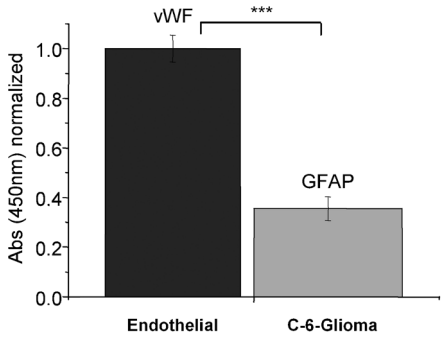

Figure 4. The relative amount of non-adhered endothelial cells and C-6-glioma cells in the supernatant determined by ELISA. The value of non-adhered cells of endothelial cells was determined to 1.000 ± 0.016 and the absolute value of C-6-glioma cells 0.333 ± 0.048. $N = 6$–8; *** data show significant differences (ANOVA one sample t-test: *** $p \leq 0.001$). The data were normalized on the absorption (450 nm) of endothelial cells to unity.

our new biocompatible surface for the selective separation of malignant C-6-glioma cell lines from primary endothelial cells.

The results open new perspectives for the construction of suitable enantiomorphous SAM of NPs (as ECM models) to understand cell–surface interactions more in detail. Furthermore, not only the control of cellular behavior (for example, cell separation, cell adhesion, cell growth, cell differentiation), but also the realization of new biocompatible surfaces for, for example, tissue engineering is envisaged.

Experimental Section

Disk-shaped zeolite L crystals were synthesized according to literature procedure[11] and the XRD pattern of zeolite L was compared with the literature results.[25] Amino functionalization,[20] DXP loading,[19] and preparation of SAMs of zeolites on glass[15a,16a] were carried out according to literature methods. Cell and ELISA experiments are described in the Supporting Information.

D- or L-PEN functionalization of zeolite L: A solution of D- or L-PEN (0.2 mM), EDC (1.5 mM), and NHS (3.0 mM) in 1 mL DMSO was added dropwise to a suspension of the NH_2-zeo (20 mg) in 1 mL DMSO. The reaction mixture was stirred for 18 h at room temperature. Subsequently, the suspension was centrifuged 10 min at 4400 rpm and the isolated solid was washed with DMSO (2×) and with ethanol (3×). Finally the solid was dried at room temperature.

Received: December 25, 2011
Published online: March 1, 2012

Keywords: cell adhesion · cell separation · enantiomorphous surfaces · self-assembled monolayers · zeolite L

[1] a) L. A. Liotta, K. Tryggvason, S. Garbisa, I. Hart, C. M. Foltz, S. Shafie, *Nature* **1980**, *284*, 67–68; b) K. M. Yamada, S. K. Akiyama, *Cell Membr.* **1984**, *2*, 77–148; c) S. Mwenifumbo, M. M. Stevens, *Biomed. Nanostruct.* **2008**, 225–260; d) R. O. Hynes, *Science* **2009**, *326*, 1216–1219.

[2] a) S. Zhang, *Nat. Biotechnol.* **2003**, *21*, 1171–1178; b) N. J. Gleason, C. J. Nodes, E. M. Higham, N. Guckert, I. A. Aksay, J. E. Schwarzbauer, J. D. Carbeck, *Langmuir* **2003**, *19*, 513–518; c) H. P. Zheng, M. C. Berg, M. F. Rubner, P. T. Hammond, *Langmuir* **2004**, *20*, 7215–7222; d) S. Zhang, X. Zhao, *J. Mater. Chem.* **2004**, *14*, 2082–2086; e) W. Kim, J. K. Ng, M. E. Kunitake, B. R. Conklin, P. D. Yang, *J. Am. Chem. Soc.* **2007**, *129*, 7228–7229; f) S. Wang, H. Wang, J. Jiao, K. J. Chen, G. E. Owens, K. Kamei, J. Sun, D. J. Sherman, C. P. Behrenbruch, H. Wu, H. R. Tseng, *Angew. Chem.* **2009**, *121*, 9132–9135; *Angew. Chem. Int. Ed.* **2009**, *48*, 8970–8973; g) C. G. Wilson, P. N. Sisco, F. A. Gadala-Maria, C. J. Murphy, E. C. Goldsmith, *Biomaterials* **2009**, *30*, 5639–5648; h) H. J. Bai, M. L. Shao, H. L. Gou, J. J. Xu, H. J. Chen, *Langmuir* **2009**, *25*, 10402–10407.

[3] a) J. Park, S. Bauer, K. von der Mark, P. Schmuki, *Nano Lett.* **2007**, *7*, 1686–1691; b) L. Ferreira, J. M. Karp, L. Nobre, R. Langer, *Cell Stem Cell* **2008**, *3*, 136–146.

[4] R. C. Gunawan, J. A. King, B. P. Lee, P. B. Messersmith, W. M. Miller, *Langmuir* **2007**, *23*, 10635–10643.

[5] a) I. Iwasaki, H. Maie, K. Akiyoshi, A. Kazunari, *Biomacromolecules* **2007**, *8*, 3162–3168; b) A. Carvalho de Souza, J. F. G. Vliegenthart, J. P. Kamerling, *Org. Biomol. Chem.* **2008**, *6*, 2095–2102.

[6] a) V. P. Torchilin, *Biopolymers* **2008**, *90*, 604–610; b) N. Ferrer-Miralles, E. Vazquez, A. Villaverde, *Trends Biotechnol.* **2008**, *26*, 267–275.

[7] a) B. K. Mann, A. T. Tsai, T. Scott-Burden, J. L. West, *Biomaterials* **1999**, *20*, 2281–2286; b) A. J. García, *Adv. Polym. Sci.* **2006**, *203*, 171–190; c) Z. Popović, M. Otter, G. Calzaferri, L. De Cola, *Angew. Chem.* **2007**, *119*, 6301–6304; *Angew. Chem. Int. Ed.* **2007**, *46*, 6188–6191.

[8] D. Hanein, B. Geiger, L. Addadi, *Science* **1994**, *263*, 1413–1416.

[9] a) T. Sun, D. Han, K. Riehemann, L. Chi, H. Fuchs, *J. Am. Chem. Soc.* **2007**, *129*, 1496–1497; b) X. Wang, H. Gan, T. Sun, B. Su, H. Fuchs, D. Vestweber, S. Butz, *Soft Matter* **2010**, *6*, 3851–3855.

[10] a) K. Tang, H. Gan, Y. Li, L. Chi, T. Sun, H. Fuchs, *J. Am. Chem. Soc.* **2008**, *130*, 11284–11285; b) H. Gan, K. Tang, T. Sun, M. Hirtz, Y. Li, L. Chi, S. Butz, H. Fuchs, *Angew. Chem.* **2009**, *121*, 5386–5390; *Angew. Chem. Int. Ed.* **2009**, *48*, 5282–5286; c) X. Wang, H. Gan, T. Sun, *Adv. Funct. Mater.* **2011**, *21*, 3276–3281; d) T. Sun, G. Qing, B. Sua, L. Jiang, *Chem. Soc. Rev.* **2011**, *40*, 2909–2921; e) M. Zhang, G. Qinga, T. Sun, *Chem. Soc Rev.* **2012**, *41*, 1972–1984.

[11] A. Z. Ruiz, D. Bruhwiler, T. Ban, G. Calzaferri, *Monatsh. Chem.* **2005**, *136*, 77–89.

[12] S. Mintova, S. Mo, T. Bein, *Chem. Mater.* **2001**, *13*, 901–905.

[13] T. Wang, A. Mitra, H. Wang, L. Huang, Y. Yan, *Adv. Mater.* **2001**, *13*, 1463–1466.

[14] a) A. Corma, V. Fornes, F. Rey, *Adv. Mater.* **2002**, *14*, 71–74; b) T. Yu, Y. Zhang, C. You, J. Zhuang, B. Wang, B. Liu, Y. Kang, Y. Tang, *Chem. Eur. J.* **2006**, *12*, 1137–1143; c) C. A. Strassert, M. Otter, R. Q. Albuquerque, A. Höne, Y. Vida, B. Maier, L. De Cola, *Angew. Chem.* **2009**, *121*, 8070–8073; *Angew. Chem. Int. Ed.* **2009**, *48*, 7928–7931.

[15] a) A. Zabala Ruiz, H. Li, G. Calzaferri, *Angew. Chem.* **2006**, *118*, 5408–5413; *Angew. Chem. Int. Ed.* **2006**, *45*, 5282–5287; b) J. S. Lee, H. Lim, K. Ha, H. Cheong, K. B. Yoon, *Angew. Chem.* **2006**, *118*, 5414–5418; *Angew. Chem. Int. Ed.* **2006**, *45*, 5288–5292.

[16] a) J. S. Lee, K. Ha, Y. J. Lee, K. B. Yoon, *Adv. Mater.* **2005**, *17*, 837–841; b) K. B. Yoon, *Acc. Chem. Res.* **2007**, *40*, 29–40; c) M. Zhou, B. Q. Zhang, X. F. Liu, *Chin. Sci. Bull.* **2008**, *53*, 801–816.

[17] N. S. Kehr, K. Riehemann, J. El-Gindi, A. Schäfer, H. Fuchs, H. J. Galla, L. De Cola, *Adv. Funct. Mater.* **2010**, *20*, 2248–2254.

[18] N. S. Kehr, J. El-Gindi, H. J. Galla, L. De Cola, *Microporous Mesoporous Mater.* **2011**, *144*, 9–14.

[19] G. Calzaferri, S. Huber, H. Maas, C. Minkowski, *Angew. Chem.* **2003**, *115*, 3860 – 3888; *Angew. Chem. Int. Ed.* **2003**, *42*, 3732 – 3758.
[20] S. N. Huber, G. Calzaferri, *Angew. Chem.* **2004**, *116*, 6906 – 6910; *Angew. Chem. Int. Ed.* **2004**, *43*, 6738 – 6742.
[21] a) T. Sun, H. Tan, D. Han, Q. Fu, L. Jiang, *Small* **2005**, *1*, 959 – 963; b) J. Y. Shiu, C. W. Kuo, W. T. Whang, P. Chen, *Lab Chip* **2010**, *10*, 556 – 558.
[22] a) J. F. Leary, P. Szaniszlo, T. W. Prow, L. M. Reece, N. Wang, D. M. Asmuth, *Proc. SPIE-Int. Soc. Opt. Eng.* **2002**, *4625*, 1 – 8; b) B. M. Dainiak, A. Kumar, I. Y. Galaev, B. Mattiasson, *Adv. Biochem. Eng./Biotechnol.* **2007**, *106*, 1 – 18; c) M. Kamihira, A. Kumar, *Adv. Biochem. Eng./Biotechnol.* **2007**, *106*, 173 – 193.
[23] D. Meyer, H. R. Baumgartner, *Br. J. Haematol.* **1983**, *54*, 1 – 9.
[24] S. K. Ludwin, J. C. Kosek,, L. F. Eng, *J. Comp. Neurol.* **1976**, *165*, 197 – 208.
[25] S. Megelski, G. Calzaferri, *Adv. Funct. Mater.* **2001**, *11*, 277 – 286.

